

Polymer waveguide thermo-optical switch with loss compensation based on $NaYF_4$: 18% Yb^{3+}, 2% Er^{3+}nanocrystals

Gui-Chao Xing(邢桂超), Mei-Ling Zhang(张美玲), Tong-He Sun(孙潼鹤), Yue-Wu Fu(符越吾), Ya-Li Huang(黄雅莉), Jian Shao(邵健), Jing-Rong Liu(刘静蓉), Fei Wang(王菲), Da-Ming Zhang(张大明)

Citation: Chin. Phys. B . 2018, 27(11): 114218. **doi:** 10.1088/1674-1056/27/114218
Journal homepage: http://cpb.iphy.ac.cn; http://iopscience.iop.org/cpb

What follows is a list of articles you may be interested in

All polymer asymmetric Mach-Zehnder interferometer waveguide sensor by imprinting bonding and laser polishing

Yu Liu(刘豫), Yue Sun(孙月), Yun-Ji Yi(衣云骥), Liang Tian(田亮), Yue Cao(曹悦), Chang-Ming Chen(陈长鸣), Xiao-Qiang Sun(孙小强), Da-Ming Zhang(张大明)

Chin. Phys. B . 2017, 26(12): 124215. **doi:** 10.1088/1674-1056/26/12/124215

Tunable wavelength filters using polymer long-period waveguide gratings based on metal-cladding directly defined technique

Ji-Hou Wang(王继厚), Chang-Ming Chen(陈长鸣), Yang Zheng(郑洋), Xi-Bin Wang(王希斌), Yun-Ji Yi(衣云骥), Xiao-Qiang Sun(孙小强), Fei Wang(王菲), Da-Ming Zhang(张大明)

Chin. Phys. B . 2017, 26(2): 024212. **doi:** 10.1088/1674-1056/26/2/024212

Holographic storage of three-dimensional image and data using photopolymer and polymer dispersed liquid crystal films

Hong-Yue Gao(高洪跃), Pan Liu(刘攀), Chao Zeng(曾超), Qiu-Xiang Yao(姚秋香), Zhiqiang Zheng(郑志强), Jicheng Liu(刘吉成), Huadong Zheng(郑华东), Ying-Jie Yu(于瀛洁), Zhen-Xiang Zeng(曾震湘), Tao Sun(孙涛)

Chin. Phys. B . 2016, 25(9): 094205. **doi:** 10.1088/1674-1056/25/9/094205

Random lasing in dye-doped polymer dispersed liquid crystal film

Rina Wu(乌日娜), Rui-xin Shi(史瑞新), Xiaojiao Wu(邬小娇), Jie Wu(吴杰), Qin Dai(岱钦)

Chin. Phys. B . 2016, 25(9): 094209. **doi:** 10.1088/1674-1056/25/9/094209

New pattern recognition system in the e-nose for Chinese spirit identification

Hui Zeng(曾慧), Qiang Li(李强), Yu Gu(谷宇)

Chin. Phys. B . 2016, 25(2): 024201. **doi:** 10.1088/1674-1056/25/2/024201

Polymer waveguide thermo-optical switch with loss compensation based on $NaYF_4$: 18% Yb^{3+}, 2% Er^{3+} nanocrystals*

Gui-Chao Xing(邢桂超), Mei-Ling Zhang(张美玲), Tong-He Sun(孙潼鹤), Yue-Wu Fu(符越吾), Ya-Li Huang(黄雅莉), Jian Shao(邵健), Jing-Rong Liu(刘静蓉), Fei Wang(王菲)†, and Da-Ming Zhang(张大明)

State Key Laboratory of Integrated Optoelectronics, College of Electronic Science and Engineering, Jilin University, Changchun 130012, *China*

(Received 25 April 2018; revised manuscript received 23 July 2018; published online 19 October 2018)

A polymer waveguide thermo-optical switch with loss compensation based on $NaYF_4$: 18% Yb^{3+}, 2% Er^{3+} nanocrystals, fabricated by traditional semiconductor processes, has been investigated. $NaYF_4$: 18% Yb^{3+}, 2% Er^{3+} nanocrystals were prepared by a pyrolysis method. The morphology and luminescent properties of the nanocrystals were characterized. The nanocrystals were doped into SU-8 as the core material of an optical waveguide amplifier. The size of the device was optimized for its optical and thermal fields as well as its transmission characteristics. The device was fabricated on a silica substrate by spin coating, photolithography, and wet etching. The insertion loss of the switch device is ∼ 15 dB. The rise and fall times of the device are 240 μs and 380 μs, respectively, as measured by application of a 304 Hz square wave voltage. The extinction ratio of the device is about 14 dB at an electrode-driving power of 7 mW. When the pump light power is 230 mW and the signal light power is 0.1 mW, the loss compensation of the device is 3.8 dB at a wavelength of 1530 nm. Optical devices with loss compensation have important research significance.

Keywords: $NaYF_4$: 18% Yb^{3+}, 2% Er^{3+} nanocrystals, loss compensation, polymer

PACS: 42.70.Jk, 42.60.Da, 42.79.–e, 42.79.Gn **DOI:** 10.1088/1674-1056/27/11/114218

1. Introduction

Optical devices are widely applied for realizing information transfer in the optical network quickly and effectively across all nodes, and there has been a rapid development of optical communication technology.[1–3] In optical networks, it is very important to achieve not only optical signal transmission and control functionalities, but also optical signal processing.[4–6] Optical switches are optical devices with multiple optional ports for transmission, and can perform logic conversion or physical switching of the light in an optical fiber or in an integrated optical path in an optical network; they have been widely used in optical connection parts, such as optical add-drop multiplexers (OADMs), optical cross connects (OXCs), and on-chip optical interconnects.[7–9] With the rapid development of optical fiber communication systems, the requirements for optical switches and optical switch matrices used for switching, protection switching, cross-connection, and dynamic variable light distribution are becoming even more stringent, and the capacity for device loss compensation has received significant attention in recent years. Switching is a key element in optical communication network nodes based on photonic integration technology.[10–12] Optical Mach–Zehnder interferometer (MZI) switches based on the thermo-optic (TO) effect have become important basic components of integrated optoelectronic chips. As integrated optical devices and circuits evolve, it is necessary to integrate as many components as possible into a single chip to reduce packaging costs, and therefore integration should be as high as possible. The loss of a single optical component may have a major impact on the quality of the chip, and even on its lifetime. Therefore, the amplification and compensation of optical signals are key to the development of integrated optical devices and circuits.[13–15] Recently, with the development of optical communications, rare-earth-doped polymer optical waveguide chips with optical amplification have received much attention.[16–18] $NaYF_4$ is an excellent fluoride matrix material with low phonon energy and high chemical stability. The erbium–ytterbium co-doped $NaYF_4$ nanocrystals can generate signal light of 1530 nm under 980 nm excitation, matched to a low-loss wavelength window in the spectrum of the silica fiber;[19,20] the corresponding waveguide amplifier has become a focus of research. In 2007, Dan *et al.* of Jilin University synthesized erbium–ytterbium co-doped LaF_3 nanocrystals and fabricated an optical waveguide amplifier. The gain of the device was 2.35 dB cm^{-1}.[21] In 2010, Lei *et al.* of Hong Kong City University synthesized oleic-acid-coated erbium–ytterbium co-doped $NaYF_4$ nanocrystals and doped into the KMBR® polymer to fabricate an optical waveguide amplifier. The gain of the device was 4.7 dB cm^{-1}.[22] In 2015, Jiao *et al.* of Jilin University fabricated an optical waveguide amplifier

*Project supported by the National Natural Science Foundation of China (Grant Nos. 61475061 and 61575076).

†Corresponding author. E-mail: wang_fei@jlu.edu.cn

© 2018 Chinese Physical Society and IOP Publishing Ltd

with a 3.42 dB cm^{-1} gain by synthesizing erbium–ytterbium co-doped $NaYF_4$ nanocrystals and incorporating them into the SU-8 polymer.[23] The successful fabrication of the optical waveguide amplifier makes it possible to realize loss compensation in a switch, and thus has important research significance.

In order to facilitate the development of silica fiber communication systems, in this paper, we present the successful design and fabrication of TO switch devices with loss compensation. $NaYF_4$: Er^{3+}, Yb^{3+} nanocrystals were synthesized and their morphology was characterized. The nanocrystals were doped into SU-8 as the core material of an optical waveguide amplifier. The device consists of SiO_2 as the undercladding, nanocrystal-doped SU-8 polymer as the waveguide core, PMMA as the cladding, and aluminum as the electrode material. The device uses an MZI-type structure. Since the SU-8 waveguide core material has a large thermal coefficient (-1.8×10^{-4} K^{-1}), it can effectively reduce the power consumption of the device; and using SiO_2, which has a large thermal conductivity, as a substrate can speed up the dissipation of heat and help to improve the responding speed of the device.[24,25] We used the software COMSOL to simulate the light and thermal fields of the waveguide. A TO switch with loss compensation was fabricated using traditional semiconductor processes including photolithography and development etching. The performance of the cleaved device was tested using a face-to-face coupling method.

2. Experimental section

2.1. Waveguide material preparation

In this study, $NaYF_4$: Er^{3+}, Yb^{3+} nanocrystals were synthesized as follows. $YCl_3{\cdot}6H_2O$ (0.485 g), $YbCl_3{\cdot}6H_2O$ (0.139 g), and $ErCl_3{\cdot}6H_2O$ (0.015 g) were added to a three-necked flask, and then octadecene (30 mL) and oleic acid (12 mL) were poured into the flask. The flask was placed in an oven at 100 °C for 10 min, the temperature was then raised and maintained at 150 °C for 30 min, and finally the sample was self-cooled to room temperature. The reaction system was filled with argon and stirred with a magnetic stirrer. NH_4F (0.296 g) was dissolved in methanol (20 mL), and NaOH (0.2 g) was dissolved in methanol (10 mL); the two solutions were sonicated for 1 h, and then added dropwise to the flask with continued stirring for another 1 h. The mixed liquid was maintained at a constant temperature of 50 °C for 1 h to evaporate the methanol. Next, under argon as a protective gas, the flask was heated to a constant temperature of 290 °C for 1 h and then cooled to room temperature. After the reaction, the solution was removed, and the remaining powder was repeatedly washed with recrystallization and centrifugation to collect the product nanocrystals. To prepare the core material for the waveguide, the nanocrystals were doped into SU-8 in a proportion of 0.4 wt.%.

2.2. Characterization

The synthesized $NaYF_4$: Er^{3+}, Yb^{3+} nanocrystals were characterized in terms of their morphology and emission properties. Figure 1 (a) shows the morphologies of the nanocrystals observed by transmission electron microscopy (TEM; JEOL JSM-7500F). From the figure, we can observe that the nanocrystals prepared by the above method have uniform particle size with a mean diameter of $\sim$ 12 nm. The emission characteristics of the nanocrystals were tested under excitation with a 980 nm wavelength laser. As shown in figure 1(b), the nanocrystals emitted strongly at 1530 nm.

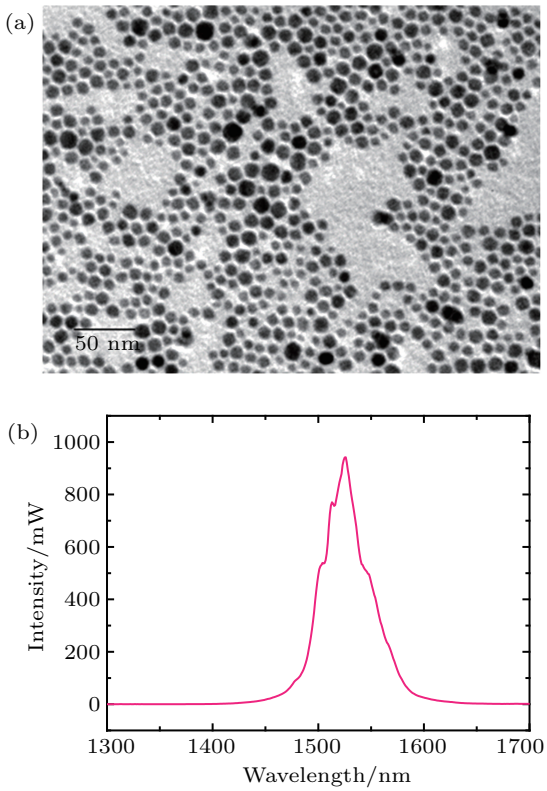


Fig. 1. (color online) (a) TEM photograph of $NaYF_4$: Er^{3+}, Yb^{3+} nanocrystals and (b) emission characteristics of the nanocrystals under 980 nm wavelength laser excitation.

2.3. Theoretical analysis and simulation

The design of the proposed TO waveguide switch is based on an MZI structure, and the specific structure is shown in figure 2(a), including the input waveguide, the Y-branch 3 dB splitter and coupler, the two interfering arms, the heater electrode, and the output waveguide. Figure 2 (b) shows a 4 μm×4 μm-sized cross-section on the top of the 5 μm SiO_2 layer that acts as a buffer for the core waveguide. The thick-

ness of the upper PMMA cladding layer is 3 μm. The aluminum electrode is placed in the waveguide within the TO active area. The principle of the TO MZI switch is as follows. When the electrode is heating, the refractive index of the polymer material of one of the interfering arms will be changed due to the TO effect, resulting in a phase difference $\Delta\Phi$ in the signal light between the two interfering arms. Through the interference of the 3 dB coupler, the two light signals are coupled and the switching state of the device is related to the phase difference $\Delta\Phi$ between the interfering arms. Therefore, the phase difference can be controlled by controlling the current flowing through the electrode, so as to control the output optical power. The temperature T dependence is given by

$$\Delta\Phi = \frac{2\pi L}{\lambda}\left(\frac{\mathrm{d}n}{\mathrm{d}T} + \alpha n\right)\Delta T,$$

where $\mathrm{d}n/\mathrm{d}T$ is the TO coefficient, α is the coefficient of thermal expansion, n is the refractive index of the TO active area, λ is the wavelength of the incident light, and L is the length of the active area. When $\Delta\Phi = \pi$, the device can be turned off.

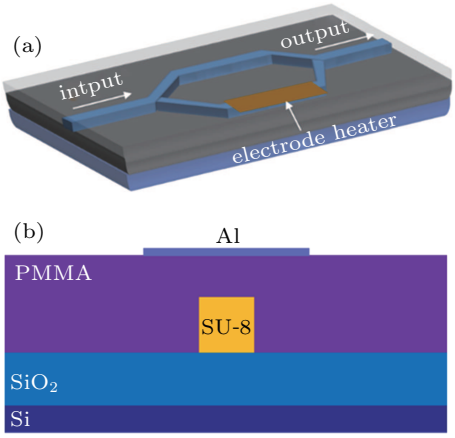


Fig. 2. (color online) Schematic representation of (a) the device and (b) its cross-section.

Taking into account the refractive index of the material and the precision of the preparation process, we designed a rectangular waveguide structure with SiO_2 ($n = 1.46$ at 1530 nm) as the under cladding, nanocrystal-doped SU-8 polymer ($n = 1.57$ at 1530 nm) as the waveguide core, PMMA ($n = 1.48$ at 1530 nm) as the upper cladding, and aluminum as the 4 μm×4 μm-sized electrode, as shown in figure 2(b). We simulated the single-mode condition of the waveguide by the effective refractive index method using Matlab software. The results show that the 4 μm × 4 μm polymer waveguide is a single mode waveguide at 1530 nm. We used the software COMSOL to simulate the distribution of optical and thermal fields within the waveguide. Figure 3(a) shows the simulation results of the optical fields distribution of the switch. The software analysis shows that 98% of the signal light power is confined within the core region. The thermal field distribution of the switching device also affects its performance. Figure 3(b) shows the simulation results of the thermal field distribution of the switch. It can be seen from the figure that the center of the core waveguide has changed by 4 K. We have

$$\Delta T = \frac{P}{LK(w/t + 0.88)},$$

where P is the electrode heating power, ΔT is the temperature difference, L is the length of the heating electrode, K is the thermal conductivity of the polymer, w is the linewidth of the electrode heater, and t is the thickness of the polymer ($P = 7$ mW, $K = 0.2$ W·K^{-1}, $L = 1$ cm, $w = 10$ μm, $t = 6$ μm). According to the above expression, the electrode driving power is about 7 mW and the temperature change at the electrode heater is 1.37 K, which are enough to make the device work.[26,27]

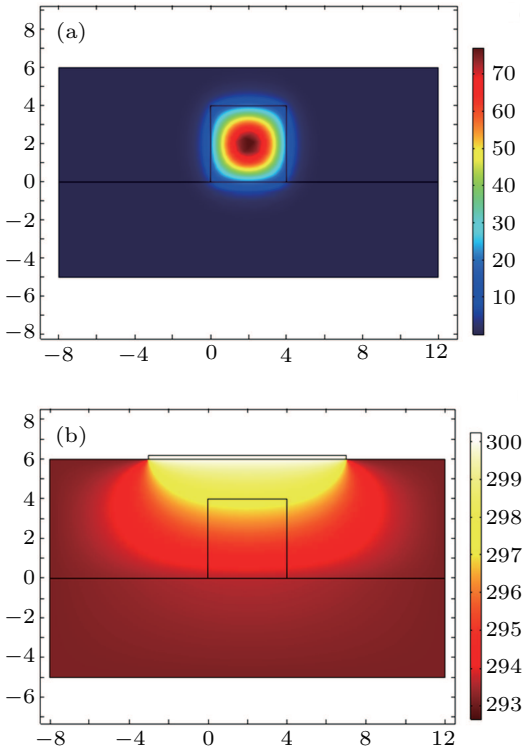


Fig. 3. (color online) Simulation distributions of (a) optical and (b) thermal fields in the waveguide.

Figure 4 shows the single-mode optical field distribution for the transverse magnetic (TM) waveguide mode simulated using Rsoft BeamPROP (Synopsys, Inc.). Figures 4(a) and 4(b) show the light field transmission simulation results at 980 nm and 1530 nm, respectively, for the case of no modulation. Figures 4(a) and 4(c), respectively, show the simulation results of the light field transmission before and after thermal modulation at the wavelength of 1530 nm.

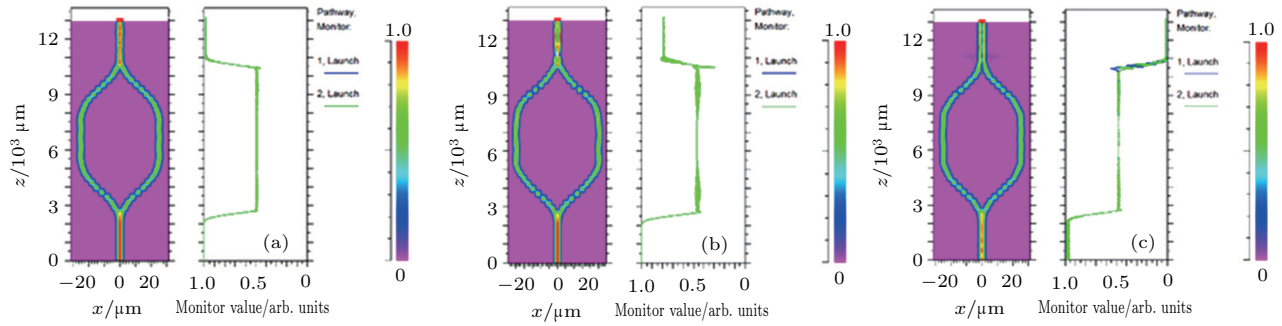


Fig. 4. (color online) Single-mode optical field distribution for the TM waveguide mode simulated by Rsoft BeamPROP: (a) before thermal modulation, at a wavelength of 1530 nm, (b) before thermal modulation, at a wavelength of 980 nm, and (c) after thermal modulation, at a wavelength of 1530 nm.

2.4. Device fabrication and testing

Figure 5(a) shows the process of preparation of the TO switch. The device may be fabricated by spin coating, lithography, deposition technologies, and wet etching, without plasma etching. Such a fabrication process is conducive to achieving large-scale multi-functional optoelectronic integrated chips at low cost, and with high compatibility and flexibility; it is also favorable for optimizing the overall performance of the chip. Figure 5(b) shows a scanning electron microscopy (SEM) image of the output waveguide cross-section without the upper cladding layer. The size of the cross-section of the waveguide is 4 μm×4 μm.

For the testing, we first cleaved the cross-section of the device and then connected the optical fiber with the optical waveguide by direct coupling. The test system arrangement is shown in figure 6. A tunable laser is used as the signal source with a wavelength range of 1510–1590 nm. A 980 nm laser is used as the pump source. The signal and pump light are coupled to a wavelength division multiplexer. The output signal light is coupled into both a photodiode detector to observe the switching response using an oscilloscope and an optical spectral analyzer (OSA, ANDO AQ-6315 A) to analyze the gain characteristics.

The relative gain of the optical waveguide amplifier is defined as

$$\text{gain} = 10\lg\left(\frac{P^{\text{p}}_{\text{s-out}}}{P_{\text{s-out}}}\right) = 10\lg(P^{\text{p}}_{\text{s-out}}) - 10\lg(P_{\text{s-out}}) \quad (\text{dB}),$$

where $P_{\text{s-out}}$ and $P^{\text{p}}_{\text{s-out}}$ are the output signal optical power without and with the presence of the pump laser light, respectively.

The test results are as follows. Figure 7(a) presents the output pattern of the device for the 1530 nm signal light. The output signal light was coupled into a photodiode detector while a square wave voltage was applied to the switched electrode heater to observe the switching response using an oscilloscope. Figure 7(b) shows the TO switching response curve observed by applying a square wave voltage of 304 Hz, with rise and fall times of 240 μs and 380 μs, respectively. The device has a good response speed, corresponding to or even faster than the input voltage signal. Figure 7(c) shows the relative gain versus pump power for different signal light powers; the pump and input signal light wavelengths were 980 nm and 1530 nm, respectively, and the signal light powers of 0.1 mW, 0.5 mW, and 1.0 mW were used. When the pump power was 230 mW and the input signal light power was 0.1 mW, the loss compensation of the device was 3.8 dB at the wavelength of 1530 nm. Figure 7(d) shows the output optical power versus electrode-driving power; the extinction ratio of the device was about 14 dB at a driving power of 7 mW. These results verify that the proposed active waveguide structure has loss compensation, reducing the insertion loss of the device, and thus can be used for manufacturing large-scale integrated devices.

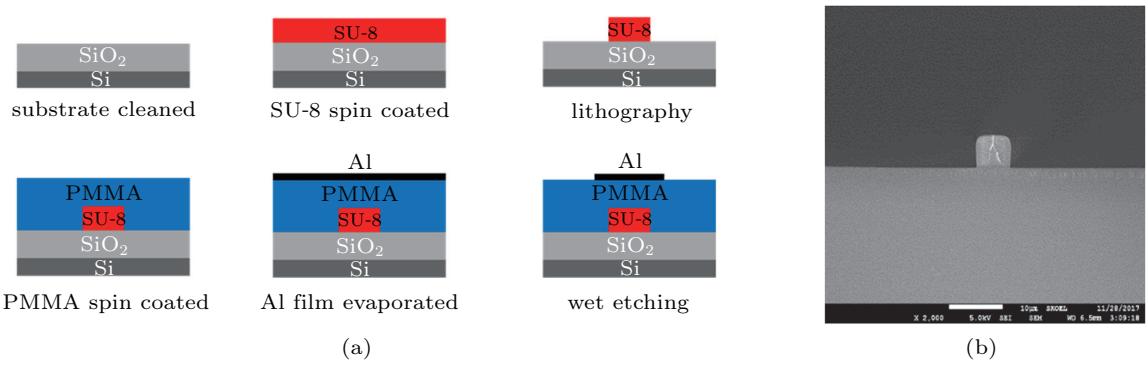


Fig. 5. (color online) (a) Preparation process of the TO switch and (b) SEM image of the waveguide cross-section.

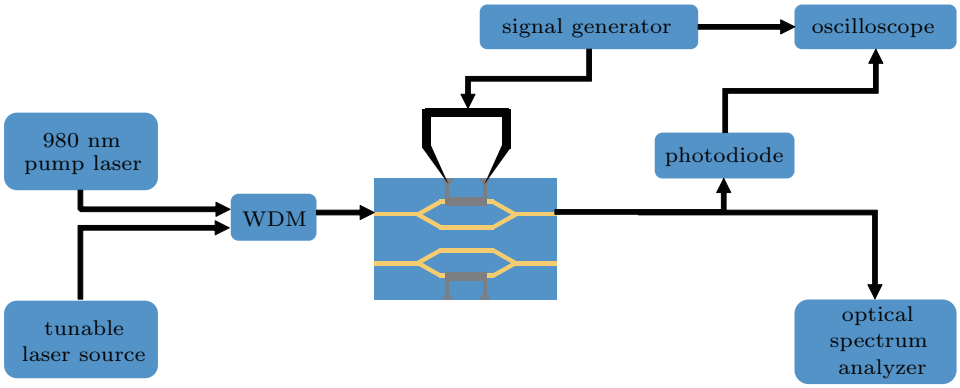


Fig. 6. (color online) Structural diagram of the test system.

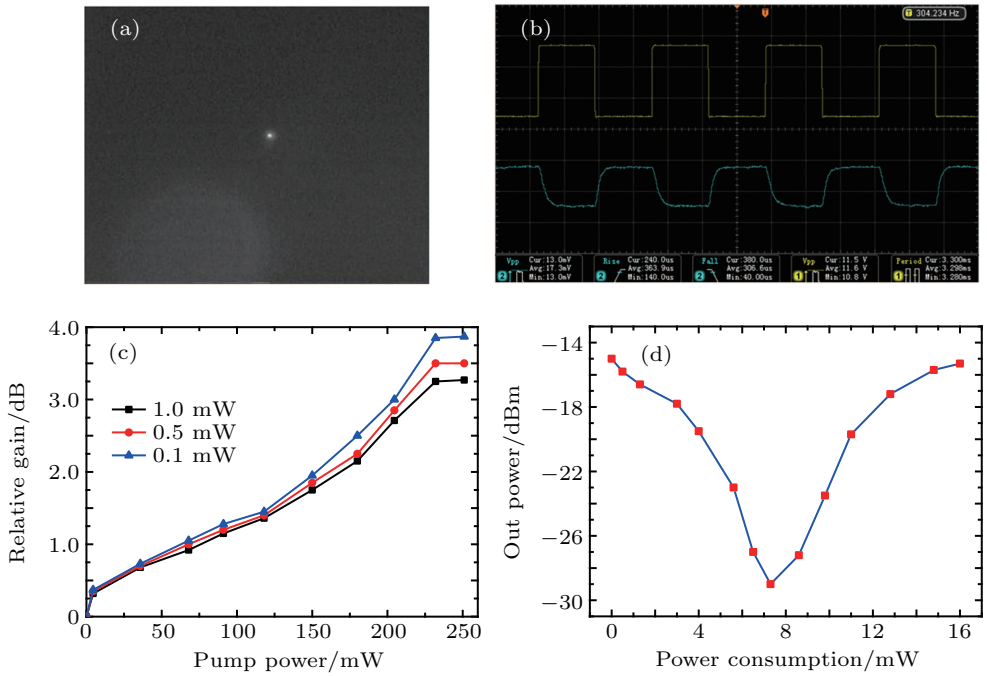


Fig. 7. (color online) (a) Output pattern of the device, (b) TO switching response curve, (c) relative gain versus pump power for different signal powers, and (d) output optical power versus driving power.

3. Conclusion

In summary, a polymer waveguide TO switch with loss compensation based on $NaYF_4$: 18% Yb^{3+}, 2% Er^{3+} nanocrystals, fabricated by traditional semiconductor processes, has been investigated. The device uses SiO_2 as the under cladding, nanocrystal-doped SU-8 polymer as the waveguide core, and PMMA as the cladding. The proposed device has a lower transmission loss and excellent TO modulation characteristics, while realizing loss compensation of the TO waveguide switch. The insertion loss of the switch device is about 15 dB. The rise and fall times of the device are 240 μs and 380 μs, respectively, as measured using a 304 Hz square wave applied voltage. The extinction ratio of the device is about 14 dB at a driving power of 7 mW. When the pump light power is 230 mW and the input signal light power is 0.1 mW, the loss compensation of the device is 3.8 dB at the wavelength of 1530 nm. If $NaYF_4$: Er^{3+}, Yb^{3+} nanocrystal polymer covalent-linking nanocomposites are used instead of physical doping to make the core material, it is expected that the concentration quenching will be reduced and the gain will be increased. Optical devices with loss compensation have important research significance. Low-loss integrated switches with loss compensation are advantageous for improving stabilities and realizing cross-connectors in large-scale photonic integrated circuits such as OADM and OXC systems.

References

[1] Gosciniak J, Markey L, Dereux A and Bozhevolnyi S I 2012 *Opt. Express* **20** 16300
[2] Bontempi F, Faralli S, Andriolli N and Contestabile G 2013 *IEEE Photon. Technol. Lett.* **25** 2178
[3] Coppola G, Sirleto L, Rendina I and Iodice M 2011 *Opt. Eng.* **50** 071112
[4] Palmer R 2014 *J. Lightwave Technol.* **32** 2726

[5] Wang J, Kroh M, Richter T, Theurer A, Matiss A, Zawadzki C, Zhang Z Y, Schubert C, Steffan A, Grote N and Keil N 2012 *IEEE Photon. Technol. Lett.* **24** 1718
[6] Chen C, Niu X Y, Han C, Shi Z, Wang X B, Sun X Q, Wang F, Cui Z and Zhang D M 2014 *Opt. Express* **22** 19895
[7] Tsang K, Wong C Y and Pun E Y B 2010 *IEEE Photonics Technol. Lett.* **22** 1024
[8] Tu Z R, Gao D S, Zhang M L and Zhang D M 2017 *Opt. Express* **25** 20911
[9] Yang B, Zhu Y, Jiao Y, He S and Dai D 2011 *J. Lightwave Technol.* **29** 2009
[10] Kim J, Lee W Y, Kang J W, Kwon S K, Kim J J and Lee J S 2001 *Macromolecules* **34** 7817
[11] Zheng Y, Chen C M, Gu Y L, Zhang D M, Cai Z Z, Shi Z S, Wang X B, Yi Y J, Sun X Q, Wang F and Cui Z C 2015 *Opt. Mater. Express* **5** 242132
[12] Zhang M L, Zhang W W, Wang F, Zhao D, Qu C Y, Wang X B, Yi Y J, Eric C and Zhang D M 2016 *Sci. Rep.* **6** 36729
[13] Zhao P C, Zhang M L, Wang T J, Liu X Y, Zhai X S, Qin G S, Qin W P, Wang F and Zhang D M 2014 *J. Nanomater.* **2014** 153028
[14] Guo R M, Wang X J, Zang K, Wang B, Wang L, Gao L F and Zhou Z P 2011 *Appl. Phys. Lett.* **99** 161115
[15] Yi Y J, Wang H R, Liu Y, Jiang M H, Wang X B, Wang F and Zhang D M 2015 *IEEE Photon. Tech. Lett.* **27** 2411
[16] Chen G F R, Zhao X Y, Sun Y, He C B, Tan M C and Tan D T H 2017 *Sci. Rep.* **7** 3366
[17] Zhao P C, Chen H Q, Zheng C T, Wang F, Zhang D M and Ma C S 2014 *Opt. Quant. Electron.* **46** 1571
[18] Wang T J, Zhao D, Zhang M L, Yin J, Song W Y, Jia Z X, Wang X B, Qin G S, Qin W P and Wang F 2015 *Opt. Mater. Express* **5** 469
[19] Naseem S, Riaz S and Sahar M R 2013 *Chin. Phys. Lett.* **30** 027301
[20] Feng S Y, Chen D P and Yu C L 2017 *Acta Phys. Sin.* **66** 164204 (in Chinese)
[21] Zhang D, Chen C, Chen C M, Ma C S, Zhang D M, Bo S H and Zhen Z 2007 *Appl. Phys. Lett.* **91** 161109
[22] Lei K L, Chow C F, Tsang K C, Lei E N Y, Roy V A L, Lam M H W, Lee C S, Pun E Y B and Li J S 2010 *J. Mater. Chem.* **20** 7526
[23] Yin J, Qu C Y, Zhang M L, Wang X B, Yi Y J, Chen C M, Sun X Q, Wang F and Zhang D M 2015 *Acta Opt. Sin.* **35** 1213001 (in Chinese)
[24] Chen C M, Wang F and Zhang D M 2012 *Chin. Phys. Lett.* **29** 014212
[25] Cao Y, Tian L and Sun Y 2017 *Chin. Phys. B* **26** 124215
[26] Schafft H A 1987 *IEEE Trans. ED* **34** 664
[27] Wang X, Howley B, Chen M Y and Chen R T J 2006 *J. Lightwave Technol.* **24** 1558